IEEE Access
Multidisciplinary ⋮ Rapid Review ⋮ Open Access Journal

Received 8 September 2023, accepted 19 September 2023, date of publication 28 September 2023,
date of current version 4 October 2023.

Digital Object Identifier 10.1109/ACCESS.2023.3320640

RESEARCH ARTICLE

Hybrid Multiple-Access: Mode Selection, User Pairing and Resource Allocation

AYSHA EBRAHIM[1], (Senior Member, IEEE), ABDULKADIR CELIK[2], (Senior Member, IEEE), EMAD ALSUSA[3], (Senior Member, IEEE), MOHAMMED W. BAIDAS[4], (Senior Member, IEEE), AND AHMED M. ELTAWIL[2], (Senior Member, IEEE)

[1]Computer Engineering Department, University of Bahrain, Sakhir Campus, Sakhir 32038, Bahrain
[2]Computer, Electrical and Mathematical Science and Engineering (CEMSE) Division, King Abdullah University of Science and Technology (KAUST), Thuwal 23955, Saudi Arabia
[3]School of Electrical and Electronic Engineering, The University of Manchester, M13 9PL Manchester, U.K.
[4]Department of Electrical Engineering, College of Engineering and Petroleum, Kuwait University, Kuwait City 13060, Kuwait

Corresponding author: Aysha Ebrahim (amebrahim@uob.edu.bh)

ABSTRACT This paper proposes hybridization of non-orthogonal multiple-access (NOMA) and orthogonal multiple access (OMA) schemes for next-generation cellular networks. Specifically, two schemes that operate NOMA/OMA mode selection as well as channel and power allocation are proposed to improve the resource utilization and bandwidth-efficiency for network capacity maximization. The two proposed hybrid schemes are: (1) single-cell hybrid multiple-access (SC-HMA) and (2) multi-cell hybrid multiple-access (MC-HMA) schemes. The SC-HMA scheme determines the optimal NOMA/OMA mode and user pairs in each resource block by utilizing a matrix representing the capacity outcomes of pairing all possible combinations of users. On the other hand, in the MC-HMA, the NOMA/OMA modes are categorized into intra-cell and inter-cell based on an interference map, where the principal objective is to determine the best mode of operation between the user pairs to improve the overall sum-rate and quality-of-service (QoS). The results show that the proposed HMA schemes provide superior overall network capacity compared to benchmark schemes. In addition, the SC-HMA scheme outperforms the MC-HMA in terms of network capacity at the expense of higher computational complexity.

INDEX TERMS Hybrid, interference management, mode selection, non-orthogonal multiple-access, resource allocation.

I. INTRODUCTION

Fifth-generation (5G) cellular networks are envisioned to support superior data rates and provide connectivity to a massive number of devices to satisfy the increasing demand for data services. In long-term evolution (LTE) and LTE-Advanced based cellular networks, orthogonal multiple-access (OMA) techniques (e.g. orthogonal frequency-division multiple-access) are utilized to allocate user equipments (UEs) different resource blocks (RBs) [1]. However, OMA schemes suffer from low spectral-efficiency as the network density increases. Therefore, in 5G applications and services—such as enhanced mobile broadband (eMBB) and massive machine-type communication (mMTC)— innovative solutions that support higher spectral-efficiency and UE density have been employed. Furthermore, non-orthogonal multiple-access (NOMA) has recently been recognized as one of the key enabling technologies to fulfill the ambitious demands of 5G+ and beyond cellular networks [2], [3]. In contrast to OMA, NOMA enables users to share the same RB simultaneously by employing superposition coding (SC) at the transmitter, and successive interference cancellation (SIC) at the receiver [4].

Despite its desirable spectral-efficiency, NOMA has been shown to deliver poorer performance than OMA in the following interference conditions [5], [6]:

1) An ideal NOMA scheme assumes that the SIC process perfectly cancels out the interference caused by the

The associate editor coordinating the review of this manuscript and approving it for publication was Olutayo O. Oyerinde.

decoded signals. In practice, however, it is possible to observe a residual interference as a result of channel estimation and decoding errors.

2) In a multi-cell NOMA network scenario, inter-cell interference (ICI) becomes a major challenge, as it can adversely affect the performance of cell-edge UEs. Indeed, ICI can significantly deteriorate the performance, especially when power allocation is ICI agnostic.

Therefore, it is desirable to be able to switch between OMA and NOMA to enhance the overall network performance under all prevailing conditions. Moreover, coordination amongst the base-stations (BSs) is necessary to mitigate ICI by power and RB allocation.

A. RELATED WORK

Recently, NOMA has been one of the most widely investigated topics due to its potential benefits. The various works on hybrid OMA and NOMA schemes can be exemplified as follows. The work in [7] investigates the performance of NOMA for massive multiple-input multiple-output (MIMO) networks, which utilizes beamforming and user clustering. The authors in [8] propose an optimal power allocation approach for hybrid NOMA/OMA and buffer-aided relay networks, while accounting for the various data rate requirements of the users. Given the high requirement for power efficiency in future wireless networks, the authors in [9] presented a power consumption based user clustering which utilizes channel conditions and inter-cell interference information to minimize each cell's power consumption. In [10], a dynamic NOMA/OMA scheme is proposed, which is performed jointly with power and subcarrier allocation. The proposed scheme utilizes a utility function that captures the trade-off between NOMA and OMA. This utility function reflects the complexity of conducting SIC as well as the complexity required to secure the minimum required bit error rate. The work in [11] presents an uplink hybrid NOMA/OMA scheme to achieve user fairness. Specifically, a fairness indicator metric based on Jain's index is introduced to provide a criterion for selecting between NOMA and OMA by characterizing the impact of individual user rates on the network sum-rate. A hybrid multiple-access (HMA) scheme based on adjusting the modulation and coding schemes (MCS) is considered in [12] to improve the network sum-capacity. In [13], a joint bandwidth control and OMA/NOMA unified network technique is proposed using a cooperative bargaining solution to maximize the network bandwidth-efficiency. The authors in [14] investigate a resource allocation problem combined with hybrid NOMA/OMA to improve the network spectral- and energy-efficiency, while incorporating quality-of-service (QoS) constraints. Outage and throughput performance of cognitive radio NOMA/OMA networks is studied in [15]. The work in [16] presents a cooperative device-to-device (D2D) with NOMA in which a BS communicates with all users simultaneously and addresses interference and weak channel conditions using novel decoding techniques. In [17], the authors investigate a multi-user dual computation offloading model in which hybrid NOMA combined with frequency division multiple access (FDMA) is utilized to improve the spectrum efficiency. The work in [18] compared the performance of a hybrid NOMA/OMA scheme and an OMA only for visible light communication (VLC) systems. The results show that a considerable performance gain can be attained with hybrid multiple access using permutation-based genetic algorithms. The authors in [19] presented a hybrid multiple access scheme for network slicing and dense mobile edge computing network. The problem is formulated to optimize the user association, resource and power allocation. The efficiency of the solution was demonstrated using extensive simulations. The work in [20] compared the performance of a hybrid NOMA/OMA scheme and an OMA only for visible light communication (VLC) systems. The results show that a considerable performance gain can be attained with hybrid multiple access using permutation-based genetic algorithms. The authors in [21] presented a hybrid multiple access scheme for network slicing and dense mobile edge-computing network. The problem is formulated to optimize the user association, resource and power allocation. The efficiency of the solution was demonstrated using extensive simulations. In [22], a distributed hybrid NOMA/OMA approach is developed for internet of things (IoT) networks. The best of both multiplexing strategies is exploited to facilitate massive connectivity of IoT devices with limited resources. The authors in [23] presented an adaptive NOMA/OMA scheme to enhance the spectral efficiency and satisfy the requirements of 6G networks.

On the other hand, many existing research works have investigated resource allocation and clustering in NOMA networks. For instance, the work in [24] proposes a method for improving the quality-of-experience (QoE) of users in multi-cell NOMA networks by optimizing the user association, frequency and power allocation of the network users. In [25], the authors propose a joint power and channel allocation for downlink NOMA networks to improve the sum-rate, while maintaining user fairness. The work in [26] calculates the user-specific rate requirements for each subchannel to select the preferred channels for different users, and then a matching game is devised for user scheduling and channel allocation. In [27], the authors examine the impact of user pairing on the sum rate performance of two different NOMA schemes: NOMA with fixed power and cognitive radio assisted NOMA. In [5] and [28], the authors address cluster formation and power-bandwidth allocation for imperfect NOMA-based downlink heterogeneous networks. Similarly, the work in [6] and [29] deals with uplink resource allocation and user pairing, and obtains the largest feasible NOMA cluster size as a function of QoS requirements, SIC efficiency, and allocated bandwidth. MIMO NOMA scenarios are considered in [30] and [31], while user

clustering for uplink NOMA networks is investigated in [32] and [33]. In [34], the authors presented a multi-cluster coordination scheme for industrial internet of things (IIoT) which provides orthogonal code, time and frequency domain multiple access for interference management. Despite their valuable contributions, the above works limit their focus on single-cell networks.

This research is motivated by the fact that hybrid NOMA/OMA combined with resource allocation in multi-cell networks has not been sufficiently addressed. Furthermore, most of the existing research use high complexity optimization methods to achieve optimal clustering whereas our research focuses on low complexity sub-optimal solutions that can achieve comparable performance in terms of resource utilization and network sum capacity.

B. CONTRIBUTIONS

To the best of the authors' knowledge, the optimal NOMA/OMA mode selection problem combined with resource allocation in multi-cell networks is still an open problem. In addition, most of the schemes in the literature assume that all the resource blocks (RBs) have identical channel gains. However, our clustering and resource allocation scheme is spectrum-aware, such that both the transmitter and receiver experience different channel quality on different RBs. To address these issues, two novel hybrid NOMA/OMA multiple access mode selection, user pairing and resource allocation schemes are proposed. The main contributions of this paper can be summarized as follows:

- The first proposed scheme is the single-cell hybrid multiple-access (SC-HMA), which is proposed for single-cell networks. In this approach, a 3D capacity matrix is developed to calculate the achievable capacity from pairing all network users, which is then utilized to determine the optimal NOMA/OMA modes and UE pairs.
- Given the complexity of multi-cell networks, we developed a low-complexity multi-cell hybrid multiple-access (MC-HMA). This scheme expands and improves our work in [35] to consider different types of operational modes, namely intra-cell and inter-cell OMA and NOMA modes. The new approach searches for the optimal UE pairs that can maximize the network capacity performance, while maintaining good QoS for users.
- Comparison to benchmark schemes, including: (1) conventional OMA, where the RBs are orthogonally allocated to UEs in a round-robin fashion, (2) conventional NOMA, in which UEs only operate in NOMA mode

C. PAPER ORGANIZATION

The rest of the paper is organized as follows. Section II presents the system model, while Section III describes the problem formulation of the proposed hybrid multiple-access and resource allocation schemes. Sections IV and V discuss the SC-HMA and MC-HMA schemes, respectively. Section VI evaluates the performance of the proposed schemes, and compares them with other benchmark schemes. Finally, Section VII concludes the paper with some final remarks.

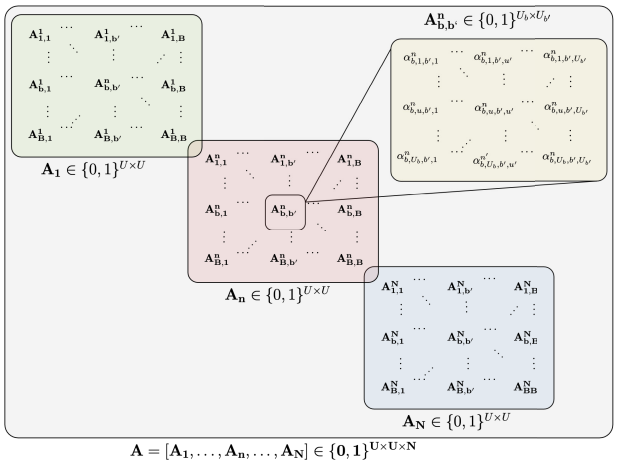

FIGURE 1. Visualization of the allocation matrix **A** and its sub-matrices.

II. NETWORK MODEL

A multi-cell downlink network of B BSs is considered in which $\mathcal{B}$ refers to a set of BSs. A group of U users are represented by the set $\mathcal{U}$, where the UEs are distributed across the network of interest in a uniform and random manner. Assume $\mathcal{U}_b$ is a group of U_b users connected with BS_b, where $\mathcal{U} = \bigcup_{b \in \mathcal{B}} \mathcal{U}_b$ and $U = \sum_{b \in \mathcal{B}} U_b$. It is assumed that there are N physical RBs, each having a bandwidth of W Hz. All BSs in the network are capable of reusing the entire set of RBs $\mathcal{N}$, in which the users are assigned in their preferred RBs according to the channel quality indicator (CQI) feedback provided by the users. Let P_T refer to BS_b total transmit power ($\forall b \in \mathcal{B}$), which is divided equally among the available RBs, where each RB has a maximum transmit power of $P_{\max} = P_T/N$.

The proposed system uses a centralized algorithm. It is assumed that the evolved packet core (EPC) acts as a central management unit where all the decisions are made and then distributed to the BSs [36]. For instance, the multiple access mode selection, the user pairing and resource allocation decisions are made by the EPC and then forwarded to the BSs.

The 3D binary RB-allocation and user-pairing matrix is denoted by $\mathbf{A} \in \{0,1\}^{U \times U \times N}$. As shown in Fig. 1, $\mathbf{A}$ can be decomposed into RB-allocation sub-matrices, i.e., $A = [A_1, \ldots, A_n, \ldots, A_N]$, where $\mathbf{A}_n \in \{0,1\}^{U \times U}$, $\forall n \in \mathcal{N}$. Also, $\mathbf{A}_n$ is the resource allocation matrix on RB_n, and consists of user-pairing sub-sub-matrices $\mathbf{A}^n_{b,b'} \in \{0,1\}^{U_b \times U_{b'}}$, $\forall (b,b') \in \mathcal{B}$. Specifically, $\mathbf{A}^n_{b,b'}$ is the user-pairing matrix between the users of BS_b and $\mathrm{BS}_{b'}$ on

RB_n, and comprises binary user-pairing elements $\alpha^n_{b,u,b',u'} \in \{0, 1\}$, which are defined as

$$\alpha^n_{b,u,b',u'} = \begin{cases} 1, & \text{if } \mathrm{RB}_n \text{ is allocated to } \mathrm{UE}_u \in \mathcal{U}_b \text{ and } \mathrm{UE}_{u'} \in \mathcal{U}_{b'}, \\ 0, & \text{otherwise.} \end{cases} \tag{1}$$

A resource block allocation and user-pairing decision can refer to a certain type of access scheme based on the BS and UE indices, which is explained as follows:

- *OMA:* Each BS_b independently allocates RB_n to $\mathrm{UE}_u \in \mathcal{U}_b$ (i.e. $u = u'$).
- *Intra-Cell (IAC)-NOMA ($b = b' \vee u \neq u'$):* BS_b pairs its users $\mathrm{UE}_u \in \mathcal{U}_b$ and $\mathrm{UE}_{u'} \in \mathcal{U}_b$, and allocates RB_n to them.
- *Inter-Cell (IRC)-NOMA ($b \neq b' \vee u \neq u'$):* BS_b and $\mathrm{BS}_{b'}$ cooperatively pair users $\mathrm{UE}_u \in \mathcal{U}_b$ and $\mathrm{UE}_{u'} \in \mathcal{U}_{b'}$, and allocate RB_n to them.

The capacity matrix associated with $\mathbf{A}$ is denoted by $\mathbf{C} \in \mathbb{R}^{U \times U \times N}$, which also follows a similar matrix structure to $\mathbf{A}$ with elements $C^n_{b,u,b',u'}$.

Throughout the paper, the superscripts b, u, and n will be used to indicate the indexes for the BSs, UEs, and RBs of interest, respectively.

A. OMA SCENARIO

Consider a scenario in which the BSs transmit signals to the UEs orthogonally over the set of available RBs. Hence, the received signal-to-interference-plus-noise ratio (SINR) of $\mathrm{UE}_u \in \mathcal{U}_b$ on RB_n (i.e. when $\alpha^n_{b,u,b,u} = 1$) is given by

$$\Gamma^n_{b,u,b,u} = \frac{P^n_{b,u} h^n_{b,u}}{\sum_{\substack{b' \in \mathcal{B} \\ b' \neq b}} \sum_{j \in \mathcal{U}_{b'}} P^n_{b',j} \alpha^n_{b',j,b',j} h^n_{b',u} + \eta}, \tag{2}$$

where $P^n_{b,u}$ denotes the power allocated to $\mathrm{UE}_u \in \mathcal{U}_b$ on RB_n, $h^n_{b,u}$ refers to the composite channel gain which considers both large- and small-scale fading, and $\eta = WN_0$ is the thermal noise power, in which N_0 refers to the noise spectral density. Moreover, the first term in the denominator denotes the inter-cell interference. Thus, the capacity of $\mathrm{UE}_u \in \mathcal{U}_b$ on RB_n is calculated as

$$C^n_{b,u,b,u} = W \cdot \log_2 \left(1 + \Gamma^n_{b,u,b,u}\right). \tag{3}$$

B. INTRA-CELL AND INTER-CELL NOMA SCENARIOS

In this section, we consider both IAC- and IRC-NOMA clustering scenarios for the NOMA scheme.

1) IAC-NOMA

An IAC-NOMA cluster is formed by pairing two different users belonging to the same BS to operate on the same RB. Assume $\mathrm{UE}_u \in \mathcal{U}_b$ and $\mathrm{UE}_{u'} \in \mathcal{U}_b$ (for $u \neq u'$), with channel gains $h^n_{b,u} > h^n_{b,u'}$. In this case, $\alpha^n_{b,u,b,u'} = 1$, and the power assigned to the users is set to $P^n_{b,u} < P^n_{b,u'}$ to guarantee that the user with the higher channel gain and lower allocated power achieves the desired SINR by canceling interference from the user with lower channel gain. Likewise, the user with lower channel gain considers the signal of the higher channel gain user as interference, which is resolved by higher power allocation.

When SIC is performed by $\mathrm{UE}_u \in \mathcal{U}_b$, some residual interference can be noticed because of the imperfect decoding of $\mathrm{UE}_{u'} \in \mathcal{U}_b$ signal, due to issues related to propagation [2]. Consequently, the SINR expressions for intra-cell clustering of UE_u and $\mathrm{UE}_{u'}$ at RB n can be expressed as [5]

$$\Gamma^n_{b,u,b,u'} = \frac{P^n_{b,u} h^n_{b,u}}{\epsilon P^n_{b,u'} h^n_{b,u} + \sum_{\substack{\{i,j\} \subseteq \mathcal{B} \\ b \notin \{i,j\}}} \sum_{\substack{k \in \mathcal{U}_i \\ l \in \mathcal{U}_j}} P^n_{i,j} \alpha^n_{i,k,j,l} h^n_{i,u} + \eta}, \tag{4}$$

and

$$\Gamma^n_{b,u',b,u} = \frac{P^n_{b,u'} h^n_{b,u'}}{P^n_{b,u} h^n_{b,u'} + \sum_{\substack{\{i,j\} \subseteq \mathcal{B} \\ b \notin \{i,j\}}} \sum_{\substack{k \in \mathcal{U}_i \\ l \in \mathcal{U}_j}} P^n_{i,j} \alpha^n_{i,k,j,l} h^n_{i,u} + \eta}, \tag{5}$$

respectively. Moreover, in (4), $0 \leq \epsilon \leq 1$ is the fractional error factor, which indicates the amount of residual interference after the SIC process. Additionally, in (5), the first and second terms of the denominator are the intra-cell and inter-cell interference terms, respectively. The SIC decodes superposed messages in the received signal in an integrative manner, where the strongest and weakest signals are decoded first and last, respectively. For a two-user case, the power reception difference between the strongest and weakest messages must be higher than the hardware sensitivity; otherwise, decoding can be erroneous since the receiver cannot distinguish between thermal noise and the message. In order to account for hardware sensitivity at the SIC receiver of $\mathrm{UE}_u \in \mathcal{U}_b$, the following constraint must be satisfied [33]

$$P^n_{b,u'} h^n_{b,u} - P^n_{b,u} h^n_{b,u} \geq \zeta, \tag{6}$$

where ζ is the hardware sensitivity.

Based on the above, the sum-capacity of $\mathrm{UE}_u \in \mathcal{U}_b$ and $\mathrm{UE}_{u'} \in \mathcal{U}_b$ is obtained as

$$C^n_{b,u,b,u'} = W \cdot \log_2 \left(1 + \Gamma^n_{b,u,b,u'}\right) + W \cdot \log_2 \left(1 + \Gamma^n_{b,u',b,u}\right). \tag{7}$$

2) IRC-NOMA

In IRC-NOMA, two users from different BSs are paired together to operate on the same RB forming a NOMA cluster. Assume $\mathrm{UE}_u \in \mathcal{U}_b$ and $\mathrm{UE}_{u'} \in \mathcal{U}_{b'}$ (for $u \neq u'$ and $b \neq b'$), with channel gains $h^n_{b,u} > h^n_{b',u'}$. In turn, $\alpha^n_{b,u,b',u'} = 1$, and the BSs coordinate to set their allocated powers as $P^n_{b,u} < P^n_{b',u'}$. Thus, the SINR expressions for inter-cell

clustering are

$$\Gamma^n_{b,u,b',u'} = \frac{P^n_{b,u} h^n_{b,u}}{\epsilon P^n_{b',u'} h^n_{b',u} + \sum\limits_{\substack{\{i,j\}\subseteq\mathcal{B} \\ \{b,b'\}\notin\{i,j\}}} \sum\limits_{\substack{k\in\mathcal{U}_i \\ l\in\mathcal{U}_j}} P^n_{i,j}\alpha^n_{i,k,j,l} h^n_{i,u} + \eta}, \tag{8}$$

and

$$\Gamma^n_{b',u',b,u} = \frac{P^n_{b',u'} h^n_{b',u'}}{P^n_{b,u} h^n_{b,u'} + \sum\limits_{\substack{\{i,j\}\subseteq\mathcal{B} \\ \{b,b'\}\notin\{i,j\}}} \sum\limits_{\substack{k\in\mathcal{U}_i \\ l\in\mathcal{U}_j}} P^n_{i,j}\alpha^n_{i,k,j,l} h^n_{i,u'} + \eta}, \tag{9}$$

respectively. To account for SIC hardware sensitivity at $\text{UE}_u \in \mathcal{U}_b$,

$$P^n_{b',u'} h^n_{b,u} - P^n_{b,u} h^n_{b,u} \geq \zeta. \tag{10}$$

In turn, the sum-capacity of $\text{UE}_u \in \mathcal{U}_b$ and $\text{UE}_{u'} \in \mathcal{U}_{b'}$ is determined as

$$C^n_{b,u,b',u'} = W \cdot \log_2\left(1 + \Gamma^n_{b,u,b',u'}\right) + W \cdot \log_2\left(1 + \Gamma^n_{b',u',b,u}\right). \tag{11}$$

C. NETWORK CAPACITY

The network capacity of the OMA scenario is obtained as

$$C_T^{\text{OMA}} = \sum_{b\in\mathcal{B}} \sum_{u\in\mathcal{U}_b} \sum_{n\in\mathcal{N}} \alpha^n_{b,u,b,u} \cdot C^n_{b,u,b,u}. \tag{12}$$

On the other hand, the network capacity of the IAC-NOMA scenario can be expressed as

$$C_T^{\text{IAC-NOMA}} = \sum_{b\in\mathcal{B}} \sum_{\substack{\{u,u'\}\subseteq\mathcal{U}_b \\ u\neq u'}} \sum_{n\in\mathcal{N}} \alpha^n_{b,u,b,u'} \cdot C^n_{b,u,b,u'}, \tag{13}$$

while the one for the IRC-NOMA scenario is obtained as

$$C_T^{\text{IRC-NOMA}} = \sum_{\substack{\{b,b'\}\subseteq\mathcal{B} \\ b\neq b'}} \sum_{\substack{u\in\mathcal{U}_b \\ u'\in\mathcal{U}_{b'}}} \sum_{n\in\mathcal{N}} \alpha^n_{b,u,b',u'} \cdot C^n_{b,u,b',u'}. \tag{14}$$

Hence, the overall network capacity is determined as

$$C_T = C_T^{\text{OMA}} + C_T^{\text{IAC-NOMA}} + C_T^{\text{IRC-NOMA}}. \tag{15}$$

III. NOMA/OMA BASED MODE SELECTION, USER PAIRING, RESOURCE BLOCK AND POWER ALLOCATION

In this work, the aim is to maximize the network capacity via mode selection, user pairing, resource block and power allocation. To this aim, the network capacity maximization (NC-MAX) problem can be formulated as given in (16), as shown at the bottom of the page. In problem **NC-MAX**, Constraint (16b), as shown at the bottom of the page, indicates that each UE_u can be paired with at most one UE over any RB, while Constraint (16c), ensures that the total transmit power over each RB does not exceed $P_{\max}$. Constraint (16d), ensures that each UE_u satisfies the minimum rate $C_{\min}$, while Constraint (16e), ensures that if two UEs are paired over an RB, the SIC hardware sensitivity is accounted for. The last two constraints define the range of values the decision variables take.

Remark 1: Problem **NC-MAX** is a mixed-integer nonlinear programming (MINLP) problem, which is non-convex and NP-hard [37], [38], and thus is computationally-expensive.

In this work, two network scenarios are considered: (1) single-cell (SC), and (2) multi-cell (MC). The SC network consists of a single BS (i.e. $B = 1$), and hence $b = b'$, $\forall (b, b') \in \mathcal{B}$, and thus $\mathcal{U}_b = \mathcal{U}_{b'} = \mathcal{U}$. In this scenario, the clustered NOMA UEs only experience intra-cell interference (i.e. no inter-cell interference), and hence, the network UEs can be assigned RBs via OMA or IAC-NOMA only. On the other hand, the MC network may involve OMA, IAC-NOMA and IRC-NOMA clustering scenarios. Clearly, the MC network scenario is more complex than

NC-MAX: (16)

$$\underset{\mathbf{A},\mathbf{P}}{\text{maximize}} \;\; C_T = C_T^{\text{OMA}} + C_T^{\text{IAC-NOMA}} + C_T^{\text{IRC-NOMA}} \tag{16a}$$

$$\text{subject to} \sum_{b'\in\mathcal{B}} \sum_{u'\in\mathcal{U}_{b'}} \alpha^n_{b,u,b',u'} \leq 1, \quad \forall n \in \mathcal{N}, \; \forall u \in \mathcal{U}_b, \text{ and } \forall b \in \mathcal{B} \tag{16b}$$

$$\sum_{u\in\mathcal{U}_b} P^n_{b,u} \leq P_{\max}, \quad \forall n \in \mathcal{N}, \text{ and } \forall b \in \mathcal{B} \tag{16c}$$

$$\sum_{n\in\mathcal{N}} \sum_{b'\in\mathcal{B}} \sum_{u'\in\mathcal{U}_{b'}} \alpha^n_{b,u,b',u'} \cdot C^n_{b,u,b',u'} \geq C_{\min}, \quad \forall u \in \mathcal{U}_b, \text{ and } \forall b \in \mathcal{B} \tag{16d}$$

$$\alpha^n_{b,u,b',u'} \cdot \left(P^n_{b',u'} h^n_{b,u} - P^n_{b,u} h^n_{b,u} - \zeta\right) \geq 0, \quad \forall u, u' \in \mathcal{U}_b, u \neq u', \; \forall b, b' \in \mathcal{B}, \text{ and } \forall n \in \mathcal{N} \tag{16e}$$

$$0 \leq P^n_{b,u} \leq P_{\max} \cdot \alpha^n_{b,u,b',u'}, \quad \forall u, u' \in \mathcal{U}, \; \forall n \in \mathcal{N}, \text{ and } \forall b, b' \in \mathcal{B} \tag{16f}$$

$$\alpha^n_{b,u,b',u'} \in \{0, 1\}, \quad \forall u, u' \in \mathcal{U}, \; \forall b, b' \in \mathcal{B}, \text{ and } \forall n \in \mathcal{N}. \tag{16g}$$

its SC counterpart scenario, which is due to the inter-cell interference terms. Thus, an algorithmic solution is proposed to solve problem **NC-MAX** for each network scenario. The first scheme, namely SC-HMA, provides the optimal network sum-rate at the expense of higher computational-complexity, while the second scheme (i.e. MC-HMA) yields a sub-optimal network sum-rate performance, but with lower computational-complexity.

IV. SC-HMA

In this section, we propose an optimal solution to **NC-MAX** problem using the novel algorithmic SC-HMA scheme. Particularly, a 3D capacity matrix $\mathbf{C} \in \mathbb{R}^{U\times U\times N}$ is constructed, and the elements of $\mathbf{C}$ are obtained by calculating the resulting capacity of all possible UE pairs over each RB. Particularly, consider the UE pair (u, u') over RB n (i.e. $\alpha^n_{b,u,b,u'} = 1$). Then, the sum-capacity maximization for this NOMA pair is determined as

$$\underset{P^n_{b,u},P^n_{b,u}}{\text{maximize}}\ C^n_{T,b,u,u'} = C^n_{b,u,u'} + C^n_{b,u',u} \tag{17}$$

$$\text{subject to } P^n_{b,u} + P^n_{b,u'} \le P_{\max} \tag{17a}$$

$$C^n_{b,u,u'}, C^n_{b,u',u} \ge C_{\min} \tag{17b}$$

$$P^n_{b,u'} h^n_{b,u} - P^n_{b,u} h^n_{b,u} \ge \zeta \tag{17c}$$

$$0 \le P^n_{b,u}, P^n_{b,u'} \le P_{\max}, \text{ for } u \ne u', \tag{17d}$$

where $C^n_{b,u,u'} = W \cdot \log_2\left(1 + \Gamma^n_{b,u,b,u'}\right)$ and $C^n_{b,u',u'} = W \cdot \log_2\left(1 + \Gamma^n_{b,u',b,u}\right)$, and $\Gamma^n_{b,u,b,u'}$ and $\Gamma^n_{b,u',b,u}$ are defined in (4) and (5), respectively. This problem can be verified to be non-convex, which is due to the non-convex rate functions. Alternatively, it can be efficiently and optimally solved via the variable substitution $P^n_{b,u} = 2^{Q^n_{b,u}}$ and $P^n_{b,u'} = 2^{Q^n_{b,u'}}$, where $Q^n_{b,u}$ and $Q^n_{b,u'}$ are respectively the transformed powers allocated to users $\text{UE}_u, \text{UE}_{u'} \in \mathcal{U}_b$ over RB_n. Additionally, a lower-bound approximation is used, where[1] $C = \log_2(1+\Gamma) \ge \omega \log_2(\Gamma) + \varpi \triangleq \bar{C}$, with $\omega = \frac{\bar{\Gamma}}{\bar{\Gamma}+1}$ and $\varpi = \log_2\left(1+\bar{\Gamma}\right) - \omega \log_2\left(\bar{\Gamma}\right)$ [39], [40]. Therefore, the sum-capacity of UEs u and u' can be lower-bounded as $C^n_{T,b,u,u'} \ge \bar{C}^n_{T,b,u,u'}$. Then, the reformulated problem (using the variable substitution and lower-bound approximation) can be verified to be a concave maximization problem for fixed values of ω and ϖ for all UEs [41]. After that, an iterative algorithm can be straightforwardly devised to solve the reformulated problem within polynomial-time complexity, while repeatedly updating the values of ω and ϖ until convergence to the optimal $P^n_{b,u}$ and $P^n_{b,u'}$ values [42].

The diagonal elements in $\mathbf{C}$ indicate the capacity achieved by selecting OMA UEs,[2] whereas the non-diagonal elements correspond to the outcome of pairing NOMA UEs (i.e. forming IAC-NOMA clusters). Algorithm 1 outlines the SC-HMA scheme. The CapacityMatrix3D function calculates the capacity matrix $\mathbf{C}$, using the allocation matrix $\mathbf{A}$. The result of this procedure is fed into the OptimalTuples procedure, which determines the optimal UE pairs over each RB, as represented by matrix $\mathbf{T}$. Finally, the Assing3D function allocates the optimal UE pairs to the selected RBs, such that the network sum-capacity is maximized.

Algorithm 1 SC-HMA

1: Set iterations index $t = 0$ and error tolerance $\varepsilon \in (0, 1)$
2: Initialize matrices $\mathbf{A}^{(0)}$, $\mathbf{C}^{(0)}$, $\mathbf{T}^{(0)}$ and calculate $C_T^{(0)}$;
3: **while** $\left|C_T^{(t)} - C_T^{(t-1)}\right| > \varepsilon$ **do**
4: $\quad\mathbf{C}^{(t)} \leftarrow \text{CapacityMatrix3D}\left(\mathbf{A}^{(t)}\right)$;
5: $\quad\mathbf{T}^{(t)} \leftarrow \text{OptimalTuples}\left(\mathbf{C}^{(t)}\right)$;
6: $\quad C_T^{(t)} \leftarrow \text{Assign3D}\left(\mathbf{C}^{(t)}, \mathbf{T}^{(t)}\right)$;
7: $\quad$ Set $t \leftarrow t + 1$;
8: **end while**
9: Return $\mathbf{A}^*$, $\mathbf{C}^*$ and $\mathbf{T}^*$;

It is assumed that the SC-HMA algorithm uses a central management unit to calculate the 3D capacity matrix-based channel state information (CSI) feedback from UEs [36]. The central unit then determines the optimal user grouping over all RBs based on the capacity matrix. The assigned resources and user pairing is then forwarded to each BS. Thus, the proposed algorithm does not add additional overhead for hybrid NOMA/OMA as all the processing and decisions are performed centrally by the 3D assignment algorithm which makes all the decisions, including the resource allocation, selection of the mode of operation (NOMA, OMA or hybrid), and power allocation based on CSI information collected from users. To be more specific, the optimal tuple obtained from the proposed 3D assignment approach determines the mode of operation. The output of this function is then communicated to the BSs, including the assigned resource blocks per user and the mode of operation.

A. 3D CAPACITY MATRIX

Algorithm 2 illustrates the procedure for calculating the 3D capacity matrix $\mathbf{C}$, where the capacity of every pair of UEs $(u, u') \in \mathcal{U}$ is calculated over each RB n. In each iteration, two conditions are checked: (a) if $u = u'$, the OMA capacity will be calculated as per (3), and (b) if $u \ne u'$, the capacity is calculated based on (7).

B. 3D ASSIGNMENT AND USER-PAIRING

The OptimalTuples function is used to optimize the frequency resource allocation of users [43]. Specifically, it uses the capacity matrix $\mathbf{C}$ to determine the optimal pair of the UEs to be allocated over all RBs. The solution to the assignment problem is approximated using a dual-primal Lagrangian relaxation technique. The 3D assignment function uses the Polyak's sub-gradient optimization algorithm [41], [43]. The OptimalTuples function generates the tuples matrix, $\mathbf{T} \in \mathbb{R}^{3\times U}$, where T(:, i) indicates the i^{th} assigned tuple (UE pair)

[1] The approximation is tight for $\Gamma = \bar{\Gamma}$, with $\Gamma, \bar{\Gamma} > 0$.

[2] It can be easily verified the capacity-maximizing power allocation problem for the OMA UEs is concave.

Algorithm 2 Calculate 3D Capacity Matrix

```
procedure CapacityMatrix3D(A)
    for u ∈ U_b and u' ∈ U_b' do
        for n ∈ N do
            if α^n_{b,u,b,u} = 1 then
                Calculate C^n_{b,u,b,u};
            else if α^n_{b,u,b,u'} = 1 then
                Calculate C^n_{b,u,b,u'};
            end if
        end for
    end for
    Return C;
end procedure
```

Algorithm 3 3D Assignment

```
T^(t) ← OptimalTuples(C^(t));
procedure Assign3D(C, T)
    for t = 1 : U do
        Get optimal UE pair and RB indexes from T(:, t);
        Assign UE pair in A;
        Update C_T;
    end for
    Return C_T;
end procedure
```

in RB_n. Note that the first two rows in T(:, i) refer to UE pair, whereas the third row is the selected RB.

The resource allocation is performed based on the optimal UE pair results generated from the OptimalTuples function. This resource assignment process is illustrated in Algorithm 3, where the Assign3D procedure takes $\mathbf{C}$ and $\mathbf{T}$ as input and generates the network sum-capacity C_T as a result. Particularly, in each iteration, the optimal UE pair over each RB is obtained from $\mathbf{T}$, and assigned in the allocation matrix $\mathbf{A}$, and then the network sum-capacity C_T is updated accordingly.

C. COMPLEXITY ANALYSIS

The complexity of Algorithm 1 is mainly determined by the cost matrix calculation and three-dimensional axial assignment (3D-AA) solution given in Algorithm 2 and Algorithm 3, respectively. The complexity of the cost matrix calculation is regulated by the number of UEs and RBs and given by $\mathcal{O}(U^2N)$.[3] On the other hand, the 3D-AA is known to be an NP-Hard problem, whose matching theory based approximate solutions can obtain results for a square cost matrix with complexity $\mathcal{O}\left(3MV^3\right)$ where M is the number of relaxations and V is the cost matrix dimensions [44]. Accordingly, the overall complexity of Algorithm 1 can be calculated as $\mathcal{O}\left(t\left(U^2N + 3MV^3\right)\right)$ where t is the number of iterations in Algorithm 1 and $V \triangleq \max(U, N)$. For the special case of $U = N$, it can be simplified as $\mathcal{O}\left(t\left(U^3 + 3MU^3\right)\right) \approx \mathcal{O}\left(3MU^3\right)$ since $t < M$ in practice.

[3]Please refer to Fig. 1 for visualization of the impact of matrix dimension on the cost matrix calculation.

V. MC-HMA

Given the complexity of multi-cell networks, a low-complexity sub-optimal algorithmic solution is proposed to solve problem **NC-MAX**. The MC-HMA algorithm builds on the techniques developed in [35] and [45] in which a multi-level interference map (MLIM) is utilized to obtain the initial OMA-based RB allocation. Then, it decides the optimal NOMA/OMA mode of operation and user pairing, which is followed by guided power allocation. Each BS calculates a local interference map based on the CSI information obtained from the associated users and then forwards this map to the central management unit. Based on this map, the central management unit computes the resources assigned to each user in the network and the user pairing for hybrid NOMA/OMA and then passes this information back to the BSs.

A. MULTI-LEVEL INTERFERENCE MAP (MLIM)

Our previous work on MLIM is employed to measure the interference intensity between the BSs, and the surrounding UEs [35]. The interference-level thresholds used to determine the interference map are defined as

$$\phi^{bu}_{lower} = \frac{\S^u_b}{\gamma_{\max}}, \tag{17}$$

and

$$\phi^{bu}_{upper} = \frac{\S^u_b}{\gamma_{\min}}, \tag{18}$$

where $\S^u_b$ is the signal strength experienced by UE_u from BS_b to which it is associated (i.e., $\S^u_b \triangleq P_b h^u_b$). Moreover, $\gamma_{\max}$ refers to the maximum supported SNR, and $\gamma_{\min}$ denotes the minimum possible SINR value for successful decoding of received messages [46]. To this end, ϕ^{bu}_{lower} represents the highest interference power that UE_u can tolerate to achieve $\gamma_{\max}$, while ϕ^{bu}_{upper} can be interpreted as the upper bound of interference experienced by UE_u, above which the interference level is classified as extremely high. Hence, the MLIM is characterized by matrix $\Phi \in \mathbb{Z}^{B\times U}$, in which the value of its elements is determined as per the interference thresholds given in (17) and (18). That is,

$$\Phi^u_{b'} = \begin{cases} 0 \text{ (low)}, & \S^u_{b'} < \phi^{bu}_{lower}, \\ 1 \text{ (mid)}, & \phi^{bu}_{lower} < \S^u_{b'} < \phi^{bu}_{upper}, \\ 2 \text{ (high)}, & \S^u_{b'} > \phi^{bu}_{upper}, \end{cases} \tag{19}$$

where $\S^u_{b'}$ represnets the received signal strength from $\text{BS}_{b'}$, for $b' \neq b$. Before allocating users ito RBs, The MLIM method classifies the interference into a number levels. In (19), the first case represents extremely low interference, in which the perceived interference from neighbouring BSs can be treated as background noise. The second case indicates tolerable interference, in which NOMA operation is feasible.

The middle case represents a moderate interference level, such that NOMA is practical. The third case refer to excessive interference in which NOMA operation is not viable.

Thus, the total number of users interfered by BS b denoted by I_b can be expressed as

$$I_b = \sum_{u \in \mathcal{U}} \left[\mathbf{1}_{\{1\}}(\Phi_b^u) + \mathbf{1}_{\{2\}}(\Phi_b^u) \right], \tag{20}$$

where $\mathbf{1}_{\{a\}}(\Phi_b^u)$ represents an indicator function which returns 1 if $a = \Phi_b^u$, and 0 otherwise, where $a \in \{1, 2\}$.

The initial values of $\alpha^n_{b,u,b',u'}$ are defined according to the MLIM in (19). These values are obtained by assigning users to RBs based on the OMA method illustrated in our previous work in [35], in which the initial amount of RBs allocated for every UE associated with BS_b is given by $N_b = \frac{N}{I_b + U_b}$. Accordingly, our proposed MC-HMA mode selection scheme is devised based on this initial RB allocation.

B. NOMA/OMA MODE SELECTION

In a multi-cell hybrid NOMA/OMA network, the effectiveness of resource utilization is defined according to two major elements: (1) The group of allocated users, and (2) The mode of operation of the allocated users (i.e. NOMA or OMA). This is characterized using a resource allocation and mode selection map $\Theta \in \mathbb{Z}^{U \times U \times N}$, with the elements $\Theta^n_{u,u'} \in \{1, 2, 3, 4\}$ which represent the following modes of operation:

Mode 1 $\left[\Theta^n_{u,u'} = 1 : \alpha^n_{b,u,b',u'} = 0\right]$**:**
This mode indicates that either UE_u or UE'_u is not allocated in RB_n. Hence, no pairing between $UE_u \in \mathcal{U}_b$ and $UE_{u'} \in \mathcal{U}_{b'}$,

Mode 2 $\left[\Theta^n_{u,u'} = 2 : (\alpha^n_{b,u,b,u} = 1) \cap (\Phi^{u'}_b = 2 \cup \Phi^u_{b'} = 2)\right]$**:**
In this mode, NOMA operation is not feasible as one of the UEs, $UE_u \in \mathcal{U}_b$ and $UE_{u'} \in \mathcal{U}_{b'}$ experience very high inter-cell interference from $BS_{b'}$ and BS_b, respectively.

Mode 3[4] $\left[\Theta^n_{u,u'} = 3 : (\alpha^n_{b,u,b',u'} = 1) \cap (\Phi^{u'}_b \oplus \Phi^u_{b'} = 1)\right]$**:**
In this mode, $UE_u \in \mathcal{U}_b$ produces tolerable interference to $UE_{u'} \in \mathcal{U}_{b'}$, while $UE_u \in \mathcal{U}_b$ receives minimal interference from $UE_{u'} \in \mathcal{U}_{b'}$, or vice versa. Therefore, the power allocated to these users can be tuned, in such a way that $UE_{u'} \in \mathcal{U}_{b'}$ cancels the interference received from $UE_u \in \mathcal{U}_b$. This mode applies for both intra-cell mode ($b = b'$) or inter-cell mode ($b \neq b'$), in which the power allocation of BSs must be coordinated according to the rules of NOMA.

Mode 4 $\left[\Theta^n_{u,u'} = 4 : (\alpha^n_{b,u,b',u'} = 1) \cap (\Phi^{u'}_b \cup \Phi^u_{b'} = 0)\right]$**:**
OMA if preferred over NOMA in this mode for the following reasons: (1) both users, $UE_u \in \mathcal{U}_b$ and $UE_{u'} \in \mathcal{U}_{b'}$ experience minimal inter-cell interference from $BS_{b'}$ and BS_b, respectively, and (2) SIC may not be successful if UE_u and UE'_u operate using NOMA since the perceived interference is weak and cannot be extracted efficiently from the superposed signal.

[4]Symbol $\oplus$ refers to XOR operator.

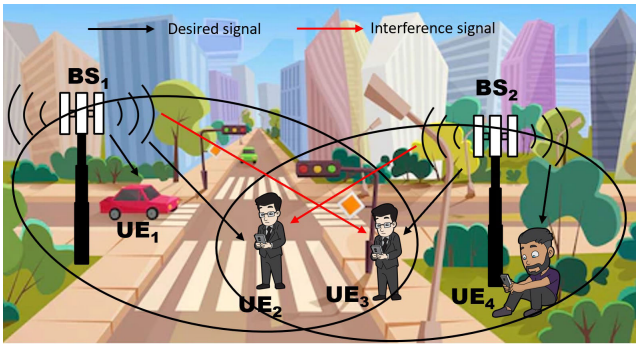

FIGURE 2. A multi-cell NOMA network for $\mathcal{U}_1 = \{1, 2\}, \mathcal{U}_2 = \{3, 4\}$.

Fig. 2 illustrates the NOMA/OMA modes of operation. We assume that UE_1 and UE_2 are associated with BS_1, and UE_3 and UE_4 are associated with BS_2. For instance, mode 2 applies if we assume that UE_2 is receiving excessive interference from BS2, then UE_2 cannot be paired with users connected to BS_2. On the other hand, users connected to the same BS can be paired in the same RB under IAC if the conditions of mode 3 are satisfied. Similarly, users belonging to different BSs can be paired under IRC based on the same mode. Moreover, users located far away from the coverage range of neighboring BSs (i.e UE_1 and UE_4) can be allocated in the same RB and operate based on OMA as explained in mode 4, since NOMA operation is not practical in this case.

C. USER PAIRING AND RESOURCE ALLOCATION

In order to locate candidate users for NOMA mode, we define two sets: (a) $\mathcal{X}_n = [1, \ldots, u, \ldots, X]$ of UEs allocated over RB n, and (b) $\mathcal{Y}_n = [1, \ldots, u', \ldots, Y]$ of UEs that are not allocated RB n, or classified to be in **Mode 2** with the UEs in $\mathcal{X}_n$. Thus, the potential NOMA pairs—from the sets $\mathcal{X}_n$ and $\mathcal{Y}_n$—are defined by the matrix $\Delta \in \{0, 1\}^{X \times Y}$, which is represented as follows

$$\Delta^n_{u,u'} = \begin{cases} 1, & \text{if } \Theta^n_{u,u'} \in \{3, 4\}, \\ 0, & \text{otherwise.} \end{cases} \tag{21}$$

After performing the initial RB allocation according to subsection V-A, the available RBs are searched to find potential users that can paired over each RB. For each u in the set $\mathcal{X}_n$, the list of candidate UEs that can be paired with UE_u over RB n is determined from the map $\Delta^n_{u,u'}$.

The following scenarios are investigated for each candidate user u':

Case 1: If u and u' are associated with the same BS (i.e. $(u, u') \in \mathcal{U}_b$), they are identified as IAC-NOMA UEs, and arranged in a descending order based on their channel gains (i.e. $h^n_{b,u} > h^n_{b,u'}$). After that, the serving BS of the high channel gain user, u, calculates the power reduction factor such that the lower interference threshold of the low channel gain user denoted by $\phi^{bu'}_{lower}$—as per (17)—is not exceeded:

$$\sigma = \S^u_b - \phi^{bu'}_{lower} \tag{22}$$

where σ represents the power reduction factor and $\S^u_b$ refers to the signal strength of UE u received by it's serving BS denoted by b. Then, BS_b allocates their transmit powers by reducing $P^n_{b,u}$ while ensuring that the total transmit power constraint is not violated as follows:

$$P^n_{b,u} = P_{\max} - \sigma \tag{23}$$

Finally, the SINR expressions for users u and u' are obtained via (4) and (5), respectively.

Case 2: If u and u' are IRC-NOMA UEs (i.e. $u \in \mathcal{U}_b$, $u' \in \mathcal{U}_{b'}$, for $b \neq b'$), then, the channel gains of the UEs are sorted in a descending order, and the BSs coordinate to adjust the transmit powers, while ensuring that $\phi^{bu'}_{lower}$ is not exceeded as illustrated in eq. (22) and (23). The SINR expressions are then calculated based on (8) and (9), respectively.

Case 3: If u and u' follow **Mode 4**, this indicates that NOMA operation is not favourable for this pair, and $UE_{u'}$'s SINR is determined based on (2).

In all cases, the candidate pair will only be allocated if the allocation leads to an improvement in the sum-capacity. The minimum capacity of users and SIC receiver sensitivity constraints must also be satisfied [5], [6].

D. COMPLEXITY AND CONVERGENCE ANALYSIS

In this section, the complexity of the MC-HMA algorithm is evaluated. The algorithm starts with OMA-Based resource allocation as explained in subsection V-A. Since this operation involves a nested loop that iterates over all BSs and their associated users, the complexity can be expressed as $O(n^2)$. The second part of the MC-HMA algorithm deals with the NOMA/OMA mode selection and user pairing. The mode selection procedure incorporates a nested loop that iterates over all available BSs and users to determine the mode of operation. Therefore, the complexity is also given by $O(n^2)$. As per user pairing, a loop iterates over all RBs to calculate the capacity achieved from the pairing process. Since the complexity of the Shannon capacity is unknown according to [47], it is assumed that its complexity is given by $O(1)$. Therefore, the complexity the capacity calculation is given by $O(n)$. Thus, the overall complexity of the MC-HMA algorithm is given by $O(n + 2n^2)$. Since the MC-HMA algorithm involves iterating over the set of available RBs to perform NOMA/OMA user pairing and capacity maximization, then, the algorithm converges after a limited number of iterations which is given by N.

VI. RESULTS AND PERFORMANCE EVALUATION

In this section, the performance of SC-HMA and MC-HMA schemes is discussed.

A. SC-HMA EVALUATION

The performance of the SC-HMA scheme is evaluated in this section and compared with the following benchmarks:

- **OMA:** This scheme assumes that the UEs operate only in the OMA mode. For fairness purposes, the OMA scheme uses the same approach discussed in algorithm 1, but with disabling the NOMA function and only allowing OMA operation.
- **NOMA:** This is a pure NOMA scheme, in which the UEs are only allowed to operate in the NOMA mode. This scheme is based on Algorithm 1 with the OMA function disabled and only allowing NOMA operation.

The simulations assume a single BS with varying number of UEs (10 to 40) and 50 RBs. The path-loss exponent is set to 2, and the shadowing variance is 4. The BS transmit power is 46 dBm, and the target minimum rate is 1×10^5 Mbps.

Table 1 depicts the impact of varying the residual interference for a network of 10 UEs on the following metrics:

- NOMA UEs: Represents the percentage of users allocated in NOMA mode.
- OMA UEs: Indicates the percentage of users allocated in OMA mode.
- Energy-Efficiency (Mbit/Joule): Total power consumption is measured by dividing the data rate by the total used power.
- Resource Utilization: The percentage of frequency resource utilization refers to the number of allocated users divided by the total available resources.

In NOMA scheme, it is shown that the percentage of NOMA UEs is 100 for all values of ϵ as a pair of users is allocated in each RB. The number of OMA UEs is 0 since UEs are not allowed to operate in OMA mode in this scheme. The percentage of resource utilization is 20% for all values of ϵ since two users are allocated in each RBs. It is also shown that the total power consumption decreases with higher values of ϵ in all schemes due to decreased data rate resulting from high values of residual interference. It is observed that the MC-HMA scheme operates in hybrid mode and that the percentage of NOMA users reduces at high values of ϵ and shifts to OMA mode when ϵ is at highest level. This shows that NOMA mode is not feasible when the residual interference is significant and therefore OMA operation is preferred. This is also the case with the SC-HMA scheme were the OMA mode is selected at high values of ϵ. This shows that the SC- and MC-HMA schemes perform the OMA/NOMA mode selection to improve the performance as

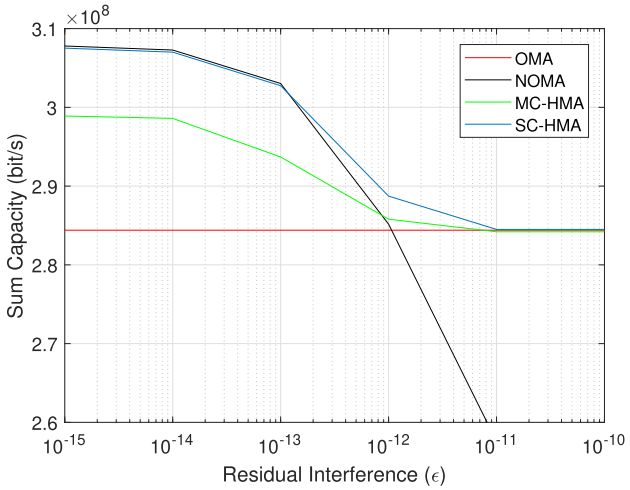

FIGURE 3. Sum-capacity with varying residual interference values.

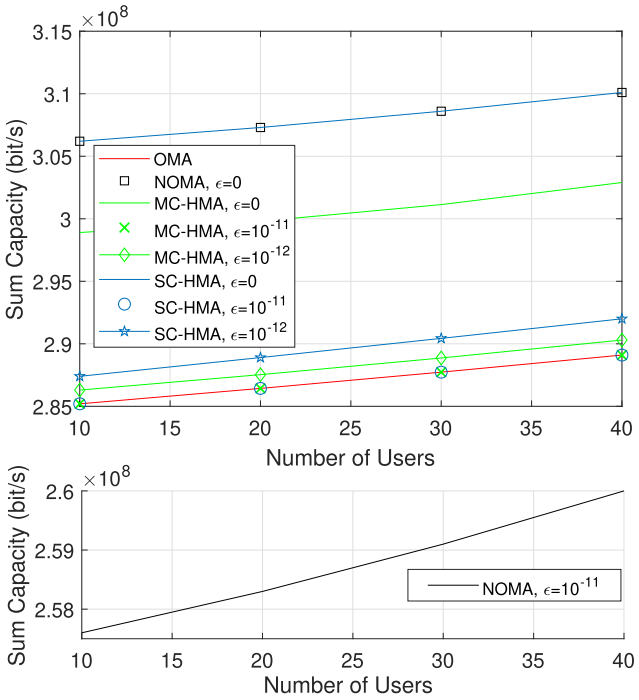

FIGURE 4. Sum-capacity with varying user densities.

will be shown in the rest of the results. It is also shown that the SC- and MC-HMA schemes prefer NOMA mode at low values of ϵ.

Fig. 3 illustrates the impact of increasing the residual interference on the sum-capacity for the SC-HMA, MC-HMA and the other benchmarks with 10 UEs. It is observed that the pure OMA is not affected by the residual interference as users operate in OMA mode only. On the other hand, the pure NOMA scheme result shows that selecting NOMA mode is not feasible at higher values of ϵ ($\geq 10^{-12}$), as this causes the sum-capacity to reduce significantly. This justifies the drop in the sum-capacity performance of the SC-HMA and MC-HMA schemes, which gradually decreases with higher values of ϵ, and starts saturating with the pure OMA scheme when $\epsilon \geq 10^{-11}$. This is because the the operation shifts to pure OMA, which proves that OMA operation outperforms NOMA at high values of ϵ.

Fig. 4 shows the network sum-capacity result with varying user densities for OMA, NOMA, SC-HMA and MC-HMA methods. It is shown that when $\epsilon = 0$, the performance of SC-HMA is similar to NOMA since the users prefer to operate in NOMA mode in the absence of residual interference. It is also seen that the sum-capacity of NOMA and SC-HMA is superior compared to the other schemes, which proves that NOMA operation improves the networks sum-capacity. The results reveal an improvement in the network sum-capacity at higher user densities due to the multi-user diversity gain, which is achieved by assigning the majority of the available resources to the users with good channel quality, where higher data rates can be achieved. The results also shows the network sum-capacity performance in the presence of residual interference. When ($\epsilon = 10^{-11}$), it is shown that the performance of SC-HMA and MC-HMA is similar to OMA, since OMA operation is more preferred when the residual interference is significant. On the other hand, the NOMA scheme performs poorly at high values of residual interference. To improve the presentation of fig. 4, the NOMA scheme at ($\epsilon = 10^{-11}$) is presented in a separate graph due to the significant performance gap compared to the other schemes.

B. MC-HMA EVALUATION

For MC-HMA evaluation, a 5 × 5 grid area is considered with an area of 10m × 10m per grid. It is presumed that UEs and Small BSs (SBS) are allocated in uniform and random positions within each grid and that there are two UEs per grid. Moreover, the total available RBs is assumed to be 25, the SBS transmit power is given by 43 dBm and the path-loss is characterized using the Terrain Type C Stanford University Interim (SUI) path-loss model [48]. The shadowing variance and the path-loss exponent are given 8 and 3 respectively.

The following benchmark schemes were used to evaluate the performance of the proposed MC-HMA method:

- **Reuse-1:** A full frequency reuse approach is considered in which every user in the network is assigned all the available RBs.
- **OMA:** In OMA method, all users are assigned equal bandwidth using round-robin scheduling algorithm.
- **MLIM:** This approach was proposed in our previous work [35].

Fig. 5 illustrates the network average data rate in comparison to the aforementioned benchmark schemes with varying cells density. It is evident that the MC-HMA scheme performs better than the other schemes in terms of average

TABLE 1. Impact of residual interference on system performance.

Scheme	Metric	Residual Interference (ϵ)					
		10^{-15}	10^{-14}	10^{-13}	10^{-12}	10^{-11}	10^{-10}
NOMA	NOMA UEs (%)	100	100	100	100	100	100
	OMA UEs (%)	0	0	0	0	0	0
	Energy-Efficiency (Mb/J)	7.73	7.71	7.61	7.16	6.47	5.67
	Resource Utilization (%)	20	20	20	20	20	20
SC-HMA	NOMA UEs (%)	100	100	100	33.1	0.7	0
	OMA UEs (%)	0	0	0	66.9	99.3	100
	Energy-Efficiency (Mb/J)	7.73	7.71	7.61	7.25	7.14	7.14
	Resource Utilization (%)	20	20	20	13.3	10.1	10
MC-HMA	NOMA UEs (%)	100	100	100	14.2	0	0
	OMA UEs (%)	0	0	0	85.8	100	100
	Energy-Efficiency (Mb/J)	7.51	7.50	7.38	7.18	7.14	7.14
	Resource Utilization (%)	20	20	20	11.4	10	10

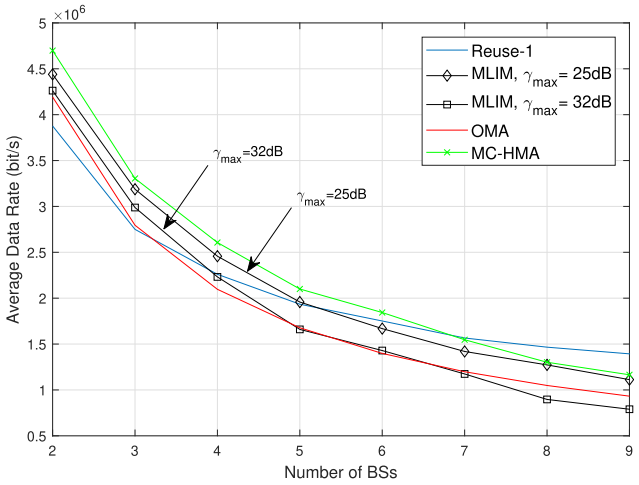

FIGURE 5. Average data rate performance with varying cell densities.

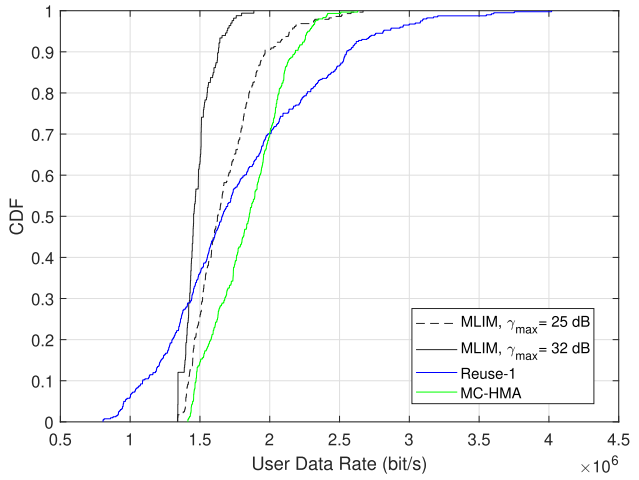

FIGURE 6. Cumulative distribution function of network throughput.

data rate. It is also noticed that lower values of $\gamma_{\max}$ in MLIM scheme lead to improvements in the average data

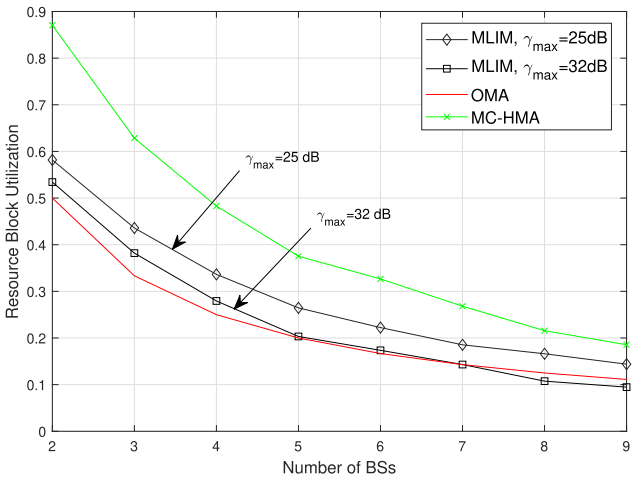

FIGURE 7. Resource block utilization performance with varying cell densities.

rate performance as the resource utilization increases when $\gamma_{\max}$ is lower. On the contrary, when $\gamma_{\max}$ is higher, the average data rate decreases as a result of lowering the frequency reuse. Furthermore, when $\gamma_{\max}$ is set to 32 dB, the performance of MLIM becomes almost comparable to OMA scheme since increasing $\gamma_{\max}$ leads to poor resource utilization as a result of users occupying orthogonal RBs. It can also be seen that the reuse-1 system performs better than the other schemes when the number of BSs is high. This is because of the high interference which leads to limiting the number of RBs assigned to each user in the other schemes. On the other hand, in reuse-1 system, the users with good channel conditions are allocated in all available RBs which improves the average data rate of the network. However, with the reuse-1 system, the cell-edge users achieve poor QoS compared to the other schemes as shown in Fig. 6 where almost 60% of the UEs achieve a data rate of less than 1.5 Mbps, while only 10% of the MC-HMA scheme

UEs achieve this data rate. This confirms that the reuse-1 system compromises the QoS of cell-edge users to improve the average network rate. Fig. 6 also shows that increasing the MC-HMA average rate does not jeopardise the QoS of users and that the QoS is improved as compared to the other schemes. The RB utilization as shown in Fig. 7 is measured by calculating the average number of utilized RBs in each BS. It is shown that the MC-HMA scheme attains the maximum RB utilization whereas the resource utilization of MLIM method can be improved by setting $\gamma_{\max}$ to lower values as illustrated previously.

VII. CONCLUSION

This paper presented novel hybrid multiple-access resource allocation schemes for improving the performance of 5G and beyond networks. The proposed SC-HMA and MC-HMA schemes focus on maximizing the network capacity and bandwidth efficiency by carefully selecting the NOMA/OMA mode of operation, which is performed jointly with resource block and power allocation. The SC-HMA, provides optimal network sum-rate at the expense of higher computational-complexity, while the MC-HMA yields a sub-optimal network sum-rate performance, but with lower computational-complexity. The performance analysis showed that the proposed approaches achieve superior results compared to the benchmark schemes.

This work can be extended in several directions. For instance, network global energy-efficiency maximization can be considered from the perspective of the single-cell and multi-cell hybrid multiple-access schemes [49]. Also, D2D-enabled communications can be studied [50], while incorporating interference management in the cellular and D2D tiers [51]. Lastly, multi-antenna selection and/or beamforming in hybrid MIMO-NOMA systems can be pursued.

REFERENCES

[1] M. Shafi, A. F. Molisch, P. J. Smith, T. Haustein, P. Zhu, P. De Silva, F. Tufvesson, A. Benjebbour, and G. Wunder, "5G: A tutorial overview of standards, trials, challenges, deployment, and practice," *IEEE J. Sel. Areas Commun.*, vol. 35, no. 6, pp. 1201–1221, Jun. 2017.

[2] Y. Liu, Z. Qin, M. Elkashlan, Z. Ding, A. Nallanathan, and L. Hanzo, "Nonorthogonal multiple access for 5G and beyond," *Proc. IEEE*, vol. 105, no. 12, pp. 2347–2381, Dec. 2017.

[3] M. Vaezi, G. A. Aruma Baduge, Y. Liu, A. Arafa, F. Fang, and Z. Ding, "Interplay between NOMA and other emerging technologies: A survey," *IEEE Trans. Cognit. Commun. Netw.*, vol. 5, no. 4, pp. 900–919, Dec. 2019.

[4] Z. Ding, Y. Liu, J. Choi, Q. Sun, M. Elkashlan, I. Chih-Lin, and H. V. Poor, "Application of non-orthogonal multiple access in LTE and 5G networks," *IEEE Commun. Mag.*, vol. 55, no. 2, pp. 185–191, Feb. 2017.

[5] A. Celik, M.-C. Tsai, R. M. Radaydeh, F. S. Al-Qahtani, and M.-S. Alouini, "Distributed cluster formation and power-bandwidth allocation for imperfect NOMA in DL-HetNets," *IEEE Trans. Commun.*, vol. 67, no. 2, pp. 1677–1692, Feb. 2019.

[6] A. Celik, M.-C. Tsai, R. M. Radaydeh, F. S. Al-Qahtani, and M.-S. Alouini, "Distributed user clustering and resource allocation for imperfect NOMA in heterogeneous networks," *IEEE Trans. Commun.*, vol. 67, no. 10, pp. 7211–7227, Oct. 2019.

[7] M. Bashar, K. Cumanan, A. G. Burr, H. Q. Ngo, L. Hanzo, and P. Xiao, "NOMA/OMA mode selection-based cell-free massive MIMO," in *Proc. IEEE Int. Conf. Commun. (ICC)*, May 2019, pp. 1–6.

[8] N. Nomikos, T. Charalambous, D. Vouyioukas, G. K. Karagiannidis, and R. Wichman, "Hybrid NOMA/OMA with buffer-aided relay selection in cooperative networks," *IEEE J. Sel. Topics Signal Process.*, vol. 13, no. 3, pp. 524–537, Jun. 2019.

[9] Y. Fu, M. Zhang, L. Salaün, C. W. Sung, and C. S. Chen, "Zero-forcing oriented power minimization for multi-cell MISO-NOMA systems: A joint user grouping, beamforming, and power control perspective," *IEEE J. Sel. Areas Commun.*, vol. 38, no. 8, pp. 1925–1940, Aug. 2020.

[10] M. Baghani, S. Parsaeefard, M. Derakhshani, and W. Saad, "Dynamic non-orthogonal multiple access and orthogonal multiple access in 5G wireless networks," *IEEE Trans. Commun.*, vol. 67, no. 9, pp. 6360–6373, Sep. 2019.

[11] Z. Wei, J. Guo, D. W. K. Ng, and J. Yuan, "Fairness comparison of uplink NOMA and OMA," in *Proc. IEEE 85th Veh. Technol. Conf. (VTC Spring)*, Jun. 2017, pp. 1–6.

[12] A. S. Marcano and H. L. Christiansen, "A novel method for improving the capacity in 5G mobile networks combining NOMA and OMA," in *Proc. IEEE 85th Veh. Technol. Conf. (VTC Spring)*, Jun. 2017, pp. 1–5.

[13] S. Kim, "Heterogeneous network bandwidth control scheme for the hybrid OMA-NOMA system platform," *IEEE Access*, vol. 8, pp. 83414–83424, 2020.

[14] Z. Song, Q. Ni, and X. Sun, "Spectrum and energy efficient resource allocation with QoS requirements for hybrid MC-NOMA 5G systems," *IEEE Access*, vol. 6, pp. 37055–37069, 2018.

[15] D.-T. Do, A.-T. Lee, and B. Lee, "On performance analysis of underlay cognitive radio-aware hybrid OMA/NOMA networks with imperfect CSI," *Electronics*, vol. 819, no. 7, pp. 1–21, 2019.

[16] Y. Ji, W. Duan, M. Wen, P. Padidar, J. Li, N. Cheng, and P.-H. Ho, "Spectral efficiency enhanced cooperative device-to-device systems with NOMA," *IEEE Trans. Intell. Transp. Syst.*, vol. 22, no. 7, pp. 4040–4050, Jul. 2021.

[17] Y. Li, Y. Wu, M. Dai, B. Lin, W. Jia, and X. Shen, "Hybrid NOMA-FDMA assisted dual computation offloading: A latency minimization approach," *IEEE Trans. Netw. Sci. Eng.*, vol. 9, no. 5, pp. 3345–3360, Sep. 2022.

[18] Z. Liu, F. Yang, J. Song, and Z. Han, "Mulitple access for downlink multi-user VLC system: NOMA or OMA user pairing?" *IEEE Wireless Commun. Lett.*, early access, Jul. 26, 2023, doi: 10.1109/LWC.2023.3299115.

[19] M. A. Hossain and N. Ansari, "Hybrid multiple access for network slicing aware mobile edge computing," *IEEE Trans. Cloud Comput.*, vol. 11, no. 3, pp. 2910–2921, Jul./Sep. 2023.

[20] Z. Liu, F. Yang, J. Song, and Z. Han, "Mulitple access for downlink multi-user VLC system: NOMA or OMA user pairing?" *IEEE Wireless Commun. Lett.*, early access, Jul. 26, 2023, doi: 10.1109/LWC.2023.3299115.

[21] M. A. Hossain and N. Ansari, "Hybrid multiple access for network slicing aware mobile edge computing," *IEEE Trans. Cloud Comput.*, vol. 11, no. 3, pp. 2910–2921, Jul./Sep. 2023.

[22] W. Lee, S. I. Choi, Y. H. Jang, and S. H. Lee, "Distributed hybrid NOMA/OMA user allocation for wireless IoT networks," *IEEE Internet Things J.*, early access, Aug. 21, 2023, doi: 10.1109/JIOT.2023.3306877.

[23] G. C. Eichler, C. G. Ralha, A. Farhang, and M. A. Marotta, "Combining NOMA-OMA with a multiagent architeture for enhanced spectrum sharing in 6G," in *Proc. IEEE/IFIP Netw. Oper. Manage. Symp. (NOMS)*, May 2023, pp. 1–7.

[24] J. Cui, Y. Liu, Z. Ding, P. Fan, and A. Nallanathan, "QoE-based resource allocation for multi-cell NOMA networks," *IEEE Trans. Wireless Commun.*, vol. 17, no. 9, pp. 6160–6176, Sep. 2018.

[25] B. Di, L. Song, and Y. Li, "Sub-channel assignment, power allocation, and user scheduling for non-orthogonal multiple access networks," *IEEE Trans. Wireless Commun.*, vol. 15, no. 11, pp. 7686–7698, Nov. 2016.

[26] B. Di, L. Song, and Y. Li, "Sub-channel assignment, power allocation, and user scheduling for non-orthogonal multiple access networks," *IEEE Trans. Wireless Commun.*, vol. 15, no. 11, pp. 7686–7698, Nov. 2016.

[27] Z. Ding, P. Fan, and H. V. Poor, "Impact of user pairing on 5G nonorthogonal multiple-access downlink transmissions," *IEEE Trans. Veh. Technol.*, vol. 65, no. 8, pp. 6010–6023, Aug. 2016.

[28] A. Celik, F. S. Al-Qahtani, R. M. Radaydeh, and M.-S. Alouini, "Cluster formation and joint power-bandwidth allocation for imperfect NOMA in DL-HetNets," in *Proc. IEEE Global Commun. Conf. (GLOBECOM)*, Dec. 2017, pp. 1–6.

[29] A. Celik, R. M. Radaydeh, F. S. Al-Qahtani, A. H. A. El-Malek, and M.-S. Alouini, "Resource allocation and cluster formation for imperfect NOMA in DL/UL decoupled HetNets," in *Proc. IEEE Globecom Workshops (GC Wkshps)*, Dec. 2017, pp. 1–6.
[30] Y. Liu, M. Elkashlan, Z. Ding, and G. K. Karagiannidis, "Fairness of user clustering in MIMO non-orthogonal multiple access systems," *IEEE Commun. Lett.*, vol. 20, no. 7, pp. 1465–1468, Jul. 2016.
[31] J. Ding, J. Cai, and C. Yi, "An improved coalition game approach for MIMO-NOMA clustering integrating beamforming and power allocation," *IEEE Trans. Veh. Technol.*, vol. 68, no. 2, pp. 1672–1687, Feb. 2019.
[32] M. A. Sedaghat and R. R. Müller, "On user pairing in uplink NOMA," *IEEE Trans. Wireless Commun.*, vol. 17, no. 5, pp. 3474–3486, May 2018.
[33] M. S. Ali, H. Tabassum, and E. Hossain, "Dynamic user clustering and power allocation for uplink and downlink non-orthogonal multiple access (NOMA) systems," *IEEE Access*, vol. 4, pp. 6325–6343, 2016.
[34] H. Zeng, J. Wang, Z. Wei, X. Zhu, Y. Jiang, Y. Wang, and C. Masouros, "Multicluster-coordination industrial Internet of Things: The era of nonorthogonal transmission," *IEEE Veh. Technol. Mag.*, vol. 17, no. 3, pp. 84–93, Sep. 2022.
[35] A. Ebrahim and E. Alsusa, "A multi-level interference mapping technique for resource management in cellular networks," in *Proc. IEEE 81st Veh. Technol. Conf. (VTC Spring)*, May 2015, pp. 1–5.
[36] E. Dahlman, S. Parkvall, and J. Skold, *4G: LTE/LTE-Advanced for Mobile Broadband*, E. Dahlman, S. Parkvall, and J. Sköld, Eds., 1st ed. USA: New York, NY, USA: Academic, 2011, pp. i–iii. [Online]. Available: https://www.sciencedirect.com/science/article/pii/B9780123854896000217, doi: 10.1016/B978-0-12-385489-6.00021-7.
[37] L. Lei, D. Yuan, C. K. Ho, and S. Sun, "Power and channel allocation for non-orthogonal multiple access in 5G systems: Tractability and computation," *IEEE Trans. Wireless Commun.*, vol. 15, no. 12, pp. 8580–8594, Dec. 2016.
[38] L. Salaün, C. S. Chen, and M. Coupechoux, "Optimal joint subcarrier and power allocation in NOMA is strongly NP-hard," in *Proc. IEEE Int. Conf. Commun. (ICC)*, May 2018, pp. 1–7.
[39] J. Papandriopoulos and J. Evans, "Low-complexity distributed algorithms for spectrum balancing in multi-user DSL networks," in *Proc. IEEE Int. Conf. Commun.*, Jun. 2006, pp. 3270–3275.
[40] J. Papandriopoulos and J. S. Evans, "SCALE: A low-complexity distributed protocol for spectrum balancing in multiuser DSL networks," *IEEE Trans. Inf. Theory*, vol. 55, no. 8, pp. 3711–3724, Aug. 2009.
[41] S. Boyd and L. Vandenberghe, *Convex Optimization*. Cambridge, U.K.: Cambridge Univ. Press, 2004.
[42] M. W. Baidas and M. R. Amini, "Resource allocation for NOMA-based multicast cognitive radio networks with energy-harvesting relays," *Phys. Commun.*, vol. 42, pp. 1–15, Oct. 2020.
[43] K. R. Pattipati, S. Deb, Y. Bar-Shalom, and R. B. Washburn, "A new relaxation algorithm and passive sensor data association," *IEEE Trans. Autom. Control*, vol. 37, no. 2, pp. 198–213, Feb. 1992.
[44] K. R. Pattipati, S. Deb, Y. Bar-Shalom, and R. B. Washburn, "A new relaxation algorithm and passive sensor data association," *IEEE Trans. Autom. Control*, vol. 37, no. 2, pp. 198–213, Feb. 1992.
[45] A. Ebrahim, A. Celik, E. Alsusa, and A. M. Eltawil, "NOMA/OMA mode selection and resource allocation for beyond 5G networks," in *Proc. IEEE 31st Annu. Int. Symp. Pers., Indoor Mobile Radio Commun.*, Aug. 2020, pp. 1–6.
[46] *Overview of 3GPP Release 12*, document TS 36.101, 3GPP, Version 0.2.0, Sep. 2015.
[47] M. Fallgren, "On the complexity of maximizing the minimum Shannon capacity in wireless networks by joint channel assignment and power allocation," in *Proc. IEEE 18th Int. Workshop Quality Service (IWQoS)*, Jun. 2010, pp. 1–7.
[48] S. S. Jeng, J. M. Chen, C. W. Tsung, and Y. F. Lu, "Coverage probability analysis of IEEE 802.16 system with smart antenna system over Stanford University interim fading channels," *IET Commun.*, vol. 4, no. 1, pp. 91–101, 2010.
[49] A. Zappone and E. Jorswieck, "Energy efficiency in wireless networks via fractional programming theory," *Found. Trends Commun. Inf. Theory*, vol. 11, nos. 3–4, pp. 185–396, 2015.
[50] M. W. Baidas, M. S. Bahbahani, E. Alsusa, K. A. Hamdi, and Z. Ding, "Joint D2D group association and channel assignment in uplink multi-cell NOMA networks: A matching-theoretic approach," *IEEE Trans. Commun.*, vol. 67, no. 12, pp. 8771–8785, Dec. 2019.
[51] M. K. Awad, M. W. Baidas, A. A. El-Amine, and N. Al-Mubarak, "A matching-theoretic approach to resource allocation in D2D-enabled downlink NOMA cellular networks," *Phys. Commun.*, vol. 54, pp. 1–22, Oct. 2022.

AYSHA EBRAHIM (Senior Member, IEEE) received the B.Sc. degree (Hons.) in computer engineering from the University of Bahrain, in 2009, the M.Sc. degree (Hons.) in electronic engineering from the University of York, in 2011, and the Ph.D. degree in electrical and electronic engineering from The University of Manchester, in 2016. She received a postgraduate certificate in academic practice (PCAP) from the University of Bahrain, in 2017. She is currently with the Department of Computer Engineering, University of Bahrain, as an Assistant Professor. Her research interests include 5G and beyond wireless networks, MAC layer design for wireless communication systems, green wireless networking, interference and radio resource management, and cloud computing. She is a fellow of the Higher Education Academy (HEA), U.K., a member of the Institute of Electrical and Electronic Engineers (IEEE), and a Board Member of the IEEE ComSoc Bahrain Chapter. In 2019, she received the Best Paper Award at the prestigious IEEE Wireless Communication and Networking Conference (IEEE WCNC 2019). She served in many IEEE events, including the organizing committee in IEEE MENACOM 2019, and the Track Chair (TPC) of Globecom'18. She has been the Chair of the Computer Engineering Department, Quality Assurance Committee, since 2018.

ABDULKADIR CELIK (Senior Member, IEEE) received the M.S. degree in electrical engineering, in 2013, the M.S. degree in computer engineering, in 2015, and the Ph.D. degree in co-majors of electrical engineering and computer engineering from Iowa State University, Ames, IA, USA, in 2016. He was a Postdoctoral Fellow with the King Abdullah University of Science and Technology, Thuwal, Saudi Arabia, from 2016 to 2020, where he is currently a Senior Research Scientist with the Communications and Computing Systems Laboratory. His research interest includes next-generation wireless communication systems and networks. He also serves as an Editor for IEEE COMMUNICATIONS LETTERS, IEEE WIRELESS COMMUNICATION LETTERS, and *Frontiers in Communications and Networks*.

EMAD ALSUSA (Senior Member, IEEE) received the Ph.D. degree in telecommunications from the University of Bath, U.K., in 2000. In 2000, he was appointed to work on developing high data rates systems as part of an industrial project based at Edinburgh University. He joined The Manchester University (then UMIST), in September 2003, as a Faculty Member, where he is currently the Head of the Communication Engineering Research Group. His research interests include communication systems with a focus on physical, MAC and network layers where applications of his research include cellular networks, the IoT, industry 4.0, radar systems, and powerline communications. His research work has resulted in over 250 journals and refereed conference publications mainly in top IEEE TRANSACTIONS and conferences. He is a fellow of the Higher Academy of Education, U.K. He received a number of awards, including the Best Paper Award at the International Symposium on Power Line Communications 2016, the Wireless Communications, Networks Conference 2019, and the IEEE International Symposium on Networks, Computers and Communications 2021. He is the TPC Track Chair of a number of conferences, such as VTC'16, GISN'16, PIMRC'17, and Globecom'18; and the General Co-Chair of the OnlineGreenCom'16 Conference. He is also the U.K. Representative of the International Union of Radio Science, and the Co-Chair of the IEEE Special Working Group on RF Energy Harvesting. He is an Editor of the IEEE WIRELESS COMMUNICATION LETTERS and IEEE TRANSACTIONS ON VEHICULAR TECHNOLOGY.

MOHAMMED W. BAIDAS (Senior Member, IEEE) received the B.Eng. degree (Hons.) in communication systems engineering from The University of Manchester, Manchester, U.K., in 2005, the M.Sc. degree (Hons.) in wireless communications engineering from the University of Leeds, Leeds, U.K., in 2006, the M.S. degree in electrical engineering from the University of Maryland, College Park, MD, USA, in 2009, and the Ph.D. degree in electrical engineering from Virginia Tech, Blacksburg, VA, USA, in 2012. He was a Visiting Researcher with The University of Manchester, from 2015 to 2016 and from 2018 to 2019. He is currently a Professor with the Department of Electrical Engineering, Kuwait University, Kuwait, where he has been with the Faculty, since May 2012. He is also a frequent reviewer of several IEEE journals and international journals and conferences, with over 95 publications. His research interests include resource allocation and management in cognitive radio systems, game theory, cooperative communications and networking, and green and energy-harvesting networks. He serves as a technical program committee member for various IEEE and international conferences. He was a recipient of the Outstanding Teaching Award from Kuwait University, from 2017 to 2018, and the Best Paper Award from the IEEE International Symposium on Networks, Computers and Communications (ISNCC2021).

AHMED M. ELTAWIL (Senior Member, IEEE) received the B.Sc. and M.Sc. degrees (Hons.) from Cairo University, Giza, Egypt, in 1997 and 1999, respectively, and the Ph.D. degree from the University of California, Los Angeles, in 2003. He is currently a Professor of electrical and computer engineering with the King Abdullah University of Science and Technology (KAUST), where he joined the Computer, Electrical and Mathematical Science and Engineering Division (CEMSE), in 2019. Prior to that, he has been with the Electrical Engineering and Computer Science Department, University of California, Irvine (UCI), since 2005. At KAUST, he is the Founder and the Director of the Communication and Computing Systems Laboratory (CCSL). His current research interests include the general area of smart and connected systems with an emphasis on mobile systems. He has been on the technical program committees and steering committees for numerous workshops, symposia, and conferences in the areas of low power computing and wireless communication system design. He is a Senior Member of the National Academy of Inventors, USA. He received several awards, including the NSF CAREER grant supporting his research in low power computing and communication systems. He received two United States Congressional certificates recognizing his contributions to research and innovation. In 2021, he was selected as the ''Innovator of the Year'' by the Henry Samueli School of Engineering, University of California, Irvine.